Improving Distribution Transformer Reliability in Micro Grids with Distributed Generation

Sondre J. K. Berg, Vijay Venu Vadlamudi, and Dimosthenis Peftitsis
Norwegian University of Science and Technology
Trondheim, Norway

***Abstract*—This paper considers a simplified microgrid derived from the CIGRE benchmark, and investigates the impact of harmonic loading of the distribution transformer on its reliability. As a means to alleviate the considerable impact of harmonics on the distribution transformer, a harmonic compensation scheme using the distributed generator inverter has been tested and found to be an efficient way of mitigating the reduced reliability of the transformer caused by harmonic loads.**

I. Introduction

One of the main challenges of low-voltage microgrids is related to the significant share of unbalanced and non-linear loads leading to distorted voltages [1], [2]. As a response to this issue, harmonic and unbalance compensation by distributed generators (DGs) has been deemed an attractive option for microgrids [1]. In recent years, several schemes for achieving power quality improvement using DGs have been proposed [1], [3]–[7]. The schemes typically adjust voltage and/or current references at harmonic frequencies, and track these by means of a resonant controller.

In [8], [9] the impact of the operational reliability of power electronics on a benchmark microgrid has been investigated, and failure rates of inverters were found to increase as a result of unbalanced compensation. Interestingly, harmonic compensation does not seem to affect the capacitor or power electronic switches in the inverter.

According to [10], the failure rate of a typical distribution transformer elsewhere is as high as $12 - 17\%$ compared to the $2 - 3\%$ (probability of failure during one year of operation) in developed countries. This causes not only a massive amount of financial costs, but also unreliability in terms of energy supplied to customers. There are many reasons for transformer failures: mechanical stress, transients, and thermal stress. Among the thermal factors causing damage to the transformer, the important ones are the operation of nonlinear load and the ambient temperature.

Among distribution transformer failures, insulation failures caused by overheating are the most common [10]. One reason for overheating and a source of de-rating of the transformer is non linear currents and voltages imposed on the transformer.

In [11], [12], harmonics are considered to hugely impact the temperature and life of transformers. In [13], dynamic rating of distribution transformers has been investigated and found that the lifetime and reliability of transformers are highly dependent on the temperature factor. In [14], the Finite Element Method-based modeling has been used to evaluate the impact of harmonic unbalanced loads, and it was found that harmonic loads would greatly increase the temperature at the same RMS current. In [15], a significant impact of harmonic loads was found on the temperature of transformer windings, resulting in degradation of insulation, and reduced lifetime and reliability. In [16], the ambient temperature and the temperature variations caused by loading have been found to considerably lower the lifetime and reliability of transformers; applying demand response has been recommended to mitigate such a situation.

The CIGRE benchmark micro grid in [17] is an LV transmission network suitable for load flow studies as well as detailed dynamic simulations and stability studies. The benchmark system contains unbalanced loads as well as distributed generation from batteries, solar- and wind power.

The rest of this paper is organised as follows: Section II gives a short summary of relevant definitions and standards. Section III introduces the transformer temperature model and the transformer reliability evaluation. Section IV describes the system used in the case study, together with its individual components. Section V presents the results of the case study, and finally section VI concludes the paper.

II. Power Quality, Definitions and reliability

According to the IEEE 519 standard [18], the Total Demand Distortion (TDD) limit is $5 - 20\%$ for odd harmonics depending on the relationship between the short circuit current I_{SC} at the Point of Common Coupling (PCC) and the maximum demand load current I_L of the system ($\frac{I_{sc}}{I_L} < 20 - \frac{I_{sc}}{I_L} > 1000$); the even harmonics limit is 25% of this.

The maximum Total Voltage Harmonic Distortion (THD_v) limit is $THD_v = 8\%$ for low voltage networks ($V_{LL} < 1kV$).

The IEEE 1547 standard [19] is also valid for microgrid systems. The TDD is defined as;

$$TDD = \frac{\sqrt{I_{rms,system}^2 - I_{1,system}^2}}{I_L} \tag{1}$$

Where $I_{rms,system}$ is the rms current, $I_{rms,1}$ is the fundamental current and I_L is the rated load demand current of the system.

Reliability is the ability of an item to perform a required function under stated conditions for a stated period of time [20]. In reliability studies, failure rates of a component can significantly affect the system-wide reliability [20], [21].

In addition to standards IEEE 1547 [19] and IEEE 519 [18], standards from the references [12] and [22] have been extensively used in the sections to follow.

III. TRANSFORMER RELIABILITY AND LIFE

A. Transformer temperature model

According to [23], the contribution of power losses from non-linear currents can be evaluated through an equivalent power frequency current I_{eq} in p.u.:

$$I_{eq} = \sqrt{\frac{P_{LL,H}}{P_{LL}}} \tag{2}$$

where P_{LL} is the power losses from the rated frequency and $P_{LL,H}$ is the power losses caused by harmonic frequencies. P_{LL} and $P_{LL,H}$ can be found as follows [23], [24]:

$$P_{LL} = P_{OL} + P_{EC} + P_{SL} \tag{3}$$

and

$$P_{LL} = P_{OL,H} + P_{EC,H} + P_{SL,H} \tag{4}$$

where P_{OL} is the ohmic losses, P_{EC} the eddy current losses, P_{SL} the magnetic flux stray losses; subscript H indicates the harmonic losses.

$$P_{OL,H} = P_{OL} \sum_{h=1}^{N} I_h^2 \tag{5}$$

$$P_{EC,H} = P_{EC} \sum_{h=1}^{N} h^2 I_h^2 \tag{6}$$

$$P_{SL,H} = P_{SL} \sum_{h=1}^{N} h^{0.8} I_h^2 \tag{7}$$

The distribution of stray losses between eddy current and magnetic stray losses depends on transformer construction and type, but is typically 50/50 for a typical ONAN transformer [22].

Furthermore, curve fitting based on measurements of 7500 transformers in [22] shows that the total load loss, $P_{LL,R}$ at rated conditions, S_R, as well as the ratio between I^2R and stray losses $P_{S,R}$ can be estimated by:

$$P_{LL,R} = 0.045 {P_R}^{0.7656} \tag{8}$$

$$P_{OL,R} = 1.0264 P_{LL,R}^{0.9435} \tag{9}$$

$$P_{SL} = 0.0308 P_{LL,R}^{1.4824} \tag{10}$$

The hot-spot temperature of a transformer can be estimated as [12]:

$$\Theta_H = \Theta_A + \Delta\Theta_{TO} + \Delta\Theta_H \tag{11}$$

$$\Delta\Theta_{TO} = (\Delta\Theta_{TO,U} - \Delta\Theta_{TO,i})\big(1 - \exp\Big\{\frac{-t}{\rho_{TO}}\Big\}\big) + \Delta\Theta_{TO,i} \tag{12}$$

$$\Delta\Theta_H = (\Delta\Theta_{H,U} - \Delta\Theta_{H,i})\big(1 - \exp\Big\{\frac{-t}{\rho_W}\Big\}\big) + \Delta\Theta_{H,i} \tag{13}$$

$$\Delta\Theta_{TO,U} = \Delta\Theta_{TO,R}(\frac{k_u^2 R + 1}{R+1})^n \tag{14}$$

$$\Delta\Theta_{TO,i} = \Delta\Theta_{TO,R}(\frac{k_i^2 R + 1}{R+1})^n \tag{15}$$

$$\Delta\Theta_{H,U} = \Delta\Theta_{H,R} k_u^{2m} \tag{16}$$

$$\Delta\Theta_{H,i} = \Delta\Theta_{H,R} k_i^{2m} \tag{17}$$

where Θ_H is the hot-spot temperature, $\Delta\Theta_{TO}$ is the top oil temperature change, $\Delta\Theta_H$ is the hot spot temperature change, R is the ratio of no-load loss to load loss at rated conditions, k is the ratio of load to rated load in pu, and m and n are constants dependent on the transformer type and cooling system.

Assuming $k = k_i = k_u$ and that Θ_A, n, m, R, $\Delta\Theta_{H,R}$ and $\Delta\Theta_{TO,R}$ are constant (in steady state), will yield a further simplified expression [25]:

$$\Theta_H = \Theta_A + \Delta\Theta_{TO,R}(\frac{k^2 R + 1}{R+1})^n + \Delta\Theta_{H,R} k^{2m} \tag{18}$$

B. Transformer lifetime and failure rate

The transformer insulation life time can be estimated as: [23], [25], [26]:

$$L_t = C \exp\left(\frac{B}{\theta_H + 273}\right) \tag{19}$$

The transformer failure rate is given by [26]:

$$\lambda(t) = \frac{\beta}{C \exp\left(\frac{B}{\theta_H + 273}\right)} \left(\frac{t}{C \exp\left(\frac{B}{\theta_H + 273}\right)}\right)^{\beta - 1} \tag{20}$$

Suppose an expected, rated lifetime L_r is known at a specific hotspot temperature $\Phi_{H,r}$. If for simplicity's sake it is assumed that an average set of conditions is causing an average hotspot temperature, then an equivalent running time, t' can thus be expressed as [26]:

$$t' = \sum \Delta t e^{\left(\frac{15000}{\Theta_{H,L_t} + 273} - \frac{15000}{\theta_{H,L_t}(t) + 273}\right)} \tag{21}$$

A weibull distribution of the failure rate can thus be given as:

$$\lambda(t) = \lambda\left(t'\right) = \frac{\beta}{L_r}\left(\frac{t'}{L_r}\right)^{\beta-1} \tag{22}$$

In [26], rated life time L_r at rated temperature $\Phi_{H,r} = 85$ is approximated to 11000 days (264k h). Shape parameter β is found to be 6.6973.

C. Validation of temperature model

The simplified temperature model in section III-A has been used to replicate and compare the results from other more advanced models, as well as with experimental results found in literature where sufficient information regarding the transformers under investigation is given.

The proposed simplified method in [12] yields an error of 3.37% when a 36 kW transformer is fed with a 1 pu fundamental current with THD of 43.4%.

The error in the temperature rise caused by a nonlinear load with $THD = 3.82\%$, compared to [11], yielded an error of 5.94%.

The estimation of the temperature in 3 experimental measurements in [11] yielded an error of $0.7 - 1.4\%$ compared to measurements performed, although without harmonics present. The transformer used was a 25 MVA, 66/11 kV, ONAF-cooled transformer.

IV. System Description

A. The microgrid

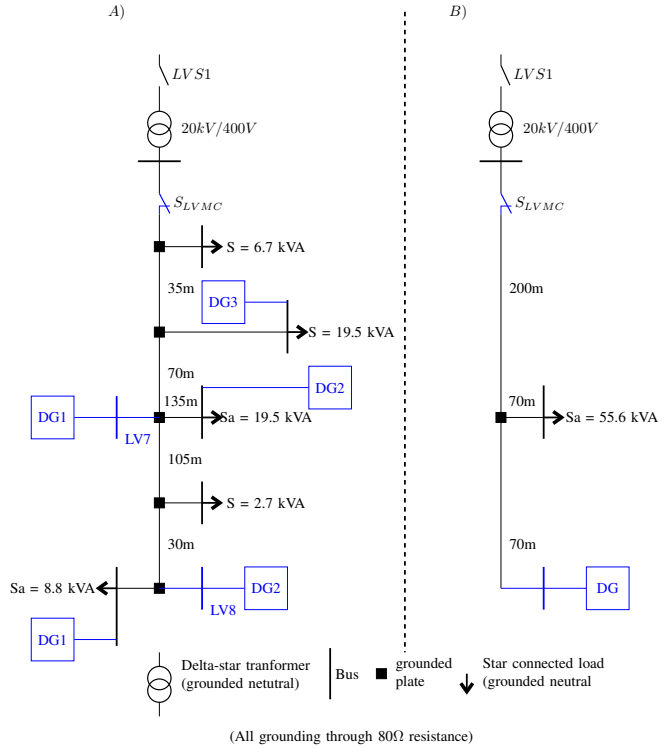

Fig. 1: CIGRE LV network: A) full system, B) lumped system

Figure 1 shows the microgrid benchmark proposed by [17] and the resulting lumped network. The microgrid is connected to the main grid through the switch LVS1. The microgrid is considered as connected to the main grid at all times in this study to investigate the transformer loading.

The line segment lengths in the lumped system are chosen so that the distance between the lumped load and the grid is equal to the mean distance per kVA of the original network. In the same manner, the length between the lumped load and DG is equal to the mean distance per kVA between DG3 and all the loads in the original system. The lumped system will thus have one DG connected where DG3 is connected in the original system.

Furthermore, the transformer parameters and the grid parameters as well as the the line parameters and the grounding scheme are taken from the CIGRE benchmark for distributed generation [17].

The lines are considered to be underground cables and the X/R ratio of line impedances set according to [17]. The grid parameters can be seen in Table II.

B. Inverter and converter model

The connected DG is represented as a 3-phase inverter connected to a constant DC source through a DC-DC dual active bridge (DAB) converter interfaced through a DC-link as shown in Fig. 2.

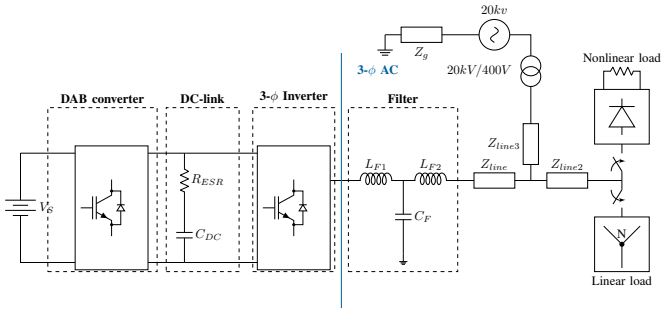

Fig. 2: Schematic diagram of lumped system with considered components.

The inverter in Fig. 1 is a 3-leg 3-phase inverter controlled with a constant active and reactive power reference. [27]. The voltage reference is tracked using cascaded voltage and current controllers, where the outer loop controls the voltage across the capacitor C_F, and the inner loop controls the current flowing through L_{F1}. Both control loops were devised in the dq frame utilizing PI controllers with appropriate decoupling terms [28]. In addition to the mentioned voltage controller, resonant controllers are added in parallel to the PI controller to reduce the steady state error at harmonic frequencies. In the dq frame the 2^{nd}, 6^{th} and 12^{th} harmonics are included. The resulting voltage controller transfer function is thus given by:

$$C_v(s) = k_{pv} + \frac{k_{iv}}{s} + \sum_{h=2,6,12} \frac{2K_h\omega_c s}{s^2 + 2\omega_c s + (h\omega_1)^2} \tag{23}$$

TABLE I: The transformer parameters

$S_R[kVA]$	$\Delta\Theta_{TO}$	$\Delta\Theta_H$	Θ_a	$\Theta_{H,R}$	[m, n]	R	$L_R[d]$
110	$35°C$	$30°C$	30	85	[0.8, 0.8]	5	11000

where k_{pv} and k_{pi} are the PI proportional and integral gains, respectively, K_h is the resonance gain corresponding to the harmonic h, ω_c is the resonant controller width and ω_1 is the angular fundamental frequency.

The distributed generator supplies a constant active power and reactive power of $30kW$ and $15kVAr$ respectively in all cases.

The dual active bridge (DAB) converters are widely used in the energy storage equipment and the distributed power systems [29]. The converter is controlled using an output voltage closed loop controller [29].

C. Loads

The load is split up into a linear load and a nonlinear load. The linear load is modelled as a constant power load. The nonlinear load is represented as a 3 phase diode rectifier. Loads have power factor of 0.85 and a total apparent power consumption of $55.6kVA$ as according to [17] and initialized using Simulink-based unbalanced load flow calculation. The algorithm uses a Newton-Raphson method and is in [30], and compared to IEEE radial distribution subcommittee's solution to 13 and 34 Node Test Feeders [31], and found to be accurate.

Five different load cases are constructed with percentages of total load drawn from the nonlinear load of 10%, 20%, 30%, 40% and 50%.

D. The transformer

The transformer used in the CIGRE benchmark [17] has 20 kV - 0.4 kV ratio and $Zeq = 0.0032 + j0.0128$ at a rated apparent power of $S_{rated} = 500kVA$. In the original system another feeder of 200 kVA is connected so the transformer is in loaded at about 50% of rated apparent power.

Assuming an ONAN cooled liquid transformer and basing its parameters from similarly rated transformers [22], [26], [32] as well as calculations from equations (8)-(10), the parameters assumed can be seen in Table I. Since these parameters are assumed based on similarly rated transformers, they will not represent one real transformer, but still provide valuable insight into what to expect from such systems given the conditions under investigation in this paper.

E. Case study

The cases considered in this study investigate the impact on transformer reliability due to harmonic current drawn from the loads in the microgrid. The cases will also consider the case of supplying harmonic compensation through the inverter of the DG. The loading condition of the transformer will also be considered as this will hugely impact the reliability. This study will consider an average set of conditions, and the failure rates for the different cases will assume the conditions of the case as constant through time. While in a real system, conditions will change continuously, this simplification will still provide insight into how much such conditions can affect the reliability of the transformer, especially since they are not considered at all in most studies.

TABLE II: The CIGRE benchmark case

Grid voltage Line-line	Grid SC power	Grid R/X ratio	Grounding resistance
400 V	5 MVA	5	80 Ω
Total load, S_L	Load power factor	DG active power, P_{DG}	DG reactive power, Q_{DG}
55.6 kVA	0.85	30 kW	15 kVAr

As such, the system will be simulated dynamically until steady state is reached for all conditions to obtain the temperature in the transformer according to section III-A. The aging failure rates will then be calculated according to section III-B assuming these conditions to be the average through all time.

The parameters in Tables I and II will be kept constant through all cases, but the percentage of load drawn from the nonlinear load will be varied from $10-50\%$, the control system of the inverter will consider both the case of no harmonic compensation as well as with harmonic compensation, and the apparent power rating of the transformer will be adjusted so the apparent load drawn corresponds to $50 - 90\%$ of the transformer rating.

Cases 1.1-5.1 thus consider a percentage of nonlinear load of 10%, 20%, 30%, 40%, and 50%, respectively, without harmonic compensation from the inverter. Cases 1.2-5.2 consider a percentage of nonlinear load of 10%, 20%, 30%, 40%, and 50%, respectively, with harmonic compensation from the inverter.

Furthermore, in the cases of harmonic compensation the voltage controller according to equation 23 is implemented in the voltage controller of the inverter.

V. Results

Figure 3 shows the current wave forms of cases 1.1, 1.5, 2.1 and 2.5, and Fig. 4 shows the Fast Fourier Transform (FFT) of all the cases.

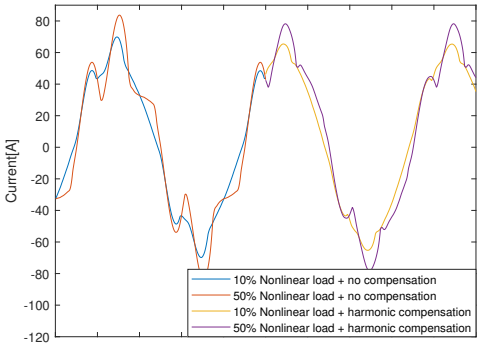

Fig. 3: The current waveform of cases 1.1, 1.5, 2.1 and 2.5.

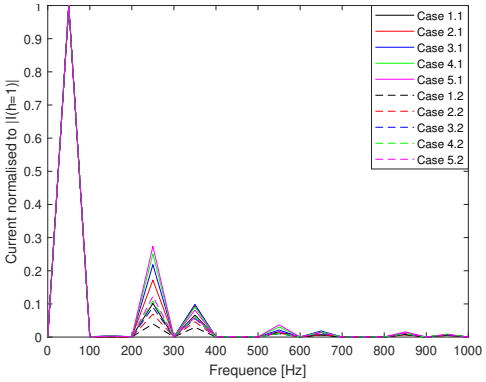

Fig. 4: The Fast Fourier Transform (FFT) of the current through the transformer of the different cases

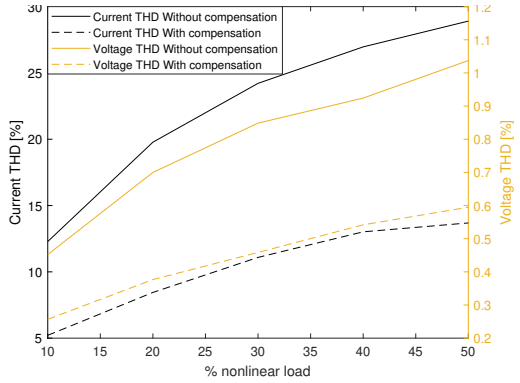

Fig. 5: The voltage and current THD of the different cases

In Fig. 5, the total harmonic distortion of the current drawn from the transformer and the voltage of the transformer both with and without harmonic compensation are shown. From this figure it is clear that that both the voltage and current THD are considerably reduced by using the harmonic compensation on the inverter. In all the cases the exact required amount of active and reactive power is supplied by the inverter.

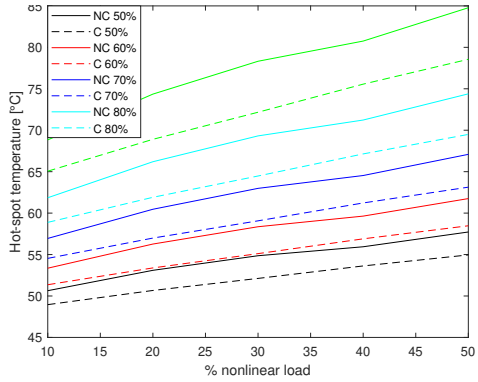

Fig. 6: The transformer hot spot temperature of the different cases. NC = no harmonic compensation, C = harmonic compensation.

As can be seen in Fig. 6, the hot-spot temperature in the transformer is heavily affected by both the loading of the transformer as well as the amount of harmonics drawn from the loads. It is also apparent that the temperature increase as a function of harmonic content is higher the more heavily loaded the transformer is.

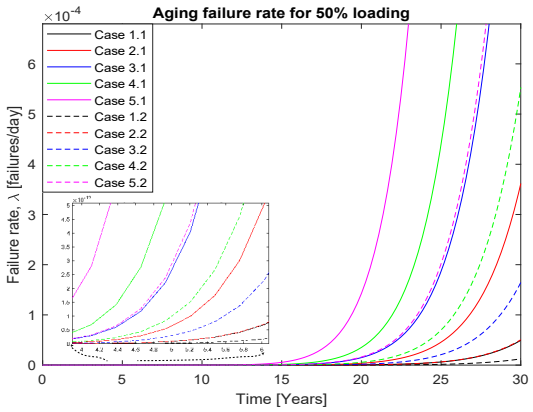

Fig. 7: The aging failure rate of the different cases when transformer is loaded at 50%

The failure rate of the transformer for 50% loading and 70% loading can be seen in Fig. 7 and Fig. 8, respectively. Several observations can be made from the results.

It is clear that the closer to the rated loading the transformer is loaded, the faster the failure rate increases and the shorter its lifetime. This is to be expected and is consistent with results from literature.

The effect of harmonic content on the failure rate and thus the reliability of the transformer is considerable, as are the improvements in reliability due to harmonic compensation from the inverter even early in the transformer lifetime. With 30% nonlinear load penetration current THD is about 10% with compensation and 25% without compensation. For the case of a 70% loaded transformer, after 5 years of operation for the 30% nonlinear load penetration, the failure rate is 20 times higher without compensation compared to the same case with compensation.

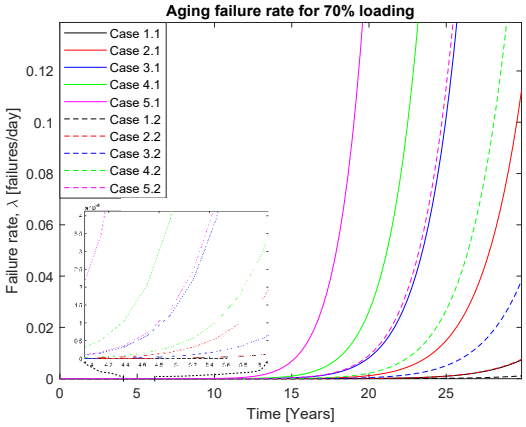

Fig. 8: The aging failure rate of the different cases when transformer is loaded at 70%

VI. Conclusions

Although often not considered in most reliability studies, the effect of harmonics on the transformer reliability is considerable. Not considering this effect can lead to misleading estimations of the microgrid reliability.

In a microgrid, the negative effects of harmonics on the transformer reliability can to a large extent be mitigated by implementing a harmonic compensation scheme in the inverter which is interfacing the DGs present in a microgrid.

References

[1] Y. W. Li and J. He, "Distribution system harmonic compensation methods: An overview of DG-interfacing inverters," *IEEE Industrial Electronics Magazine*, vol. 8, pp. 18–31, Dec 2014.

[2] J. C. Das, *Power System Harmonics and Passive Filter Designs*. John Wiley & Sons, 2015.

[3] U. Borup, F. Blaabjerg, and P. N. Enjeti, "Sharing of nonlinear load in parallel-connected three-phase converters," *IEEE Transactions on Industry Applications*, vol. 37, pp. 1817–1823, Nov 2001.

[4] D. De and V. Ramanarayanan, "Decentralized parallel operation of inverters sharing unbalanced and nonlinear loads," *IEEE Transactions on Power Electronics*, vol. 25, pp. 3015–3025, Dec 2010.

[5] P. Cheng, C. Chen, T. Lee, and S. Kuo, "A cooperative imbalance compensation method for distributed-generation interface converters," *IEEE Transactions on Industry Applications*, vol. 45, pp. 805–815, Mar 2009.

[6] X. Wang, F. Blaabjerg, Z. Chen, and J. M. Guerrero, "A centralized control architecture for harmonic voltage suppression in islanded microgrids," in *IECON 2011 - 37th Annual Conference of the IEEE Industrial Electronics Society*, pp. 3070–3075, Nov 2011.

[7] X. Wang, F. Blaabjerg, and Z. Chen, "Autonomous Control of Inverter - Interfaced Distributed Generation Units for Harmonic Current Filtering and Resonance Damping in an Islanded Microgrid," *IEEE Transactions on Industry Applications*, vol. 50, no. 1, pp. 452–461, 2014.

[8] W. Zhong, L. Wang, Z. Liu, and S. Hou, "Reliability evaluation and improvement of islanded microgrid considering operation failures of power electronic equipment," *Journal of Modern Power Systems and Clean Energy*, vol. 8, no. 1, pp. 111–123, 2020.

[9] S. J. K. Berg, F. Göthner, V. V. Vadlamudi, and D. Peftitsis, "Investigation of the effect of operating conditions on reliability of dc-link capacitors in microgrids," in *2020 IEEE PES Innovative Smart Grid Technologies Europe (ISGT-Europe)*, pp. 26–30, 2020.

[10] J. Maan and S. Singh, "Transformer failure analysis:reasons and methods," 02 2020.

[11] O. Gouda, G. Amer, and W. Salem, "Predicting transformer temperature rise and loss of life in the presence of harmonic load currents," *Ain Shams Engineering Journal*, vol. 3, no. 2, pp. 113–121, 2012.

[12] "Ieee guide for loading mineral-oil-immersed transformers and step-voltage regulators," *IEEE Std C57.91-2011 (Revision of IEEE Std C57.91-1995)*, pp. 1–123, 2012.

[13] P. Hilber, O. Ariza Rocha, K. Morozovska, T. Laneryd, O. Ivarsson, and C. Ahlrot, "Dynamic rating assists cost-effective expansion of wind farms by utilizing the hidden capacity of transformers," *International Journal of Electrical Power Energy Systems*, vol. 123, 12 2020.

[14] I. Iskender and A. Najafi, "Evaluation of transformer performance under harmonic load based on 3-d time stepping finite element method," in *2014 16th International Conference on Harmonics and Quality of Power (ICHQP)*, pp. 224–228, 2014.

[15] T. Dao and B. Phung, "Study of voltage harmonic effect on temperature rise in distribution transformer," in *2016 IEEE International Conference on Power System Technology (POWERCON)*, pp. 1–5, 2016.

[16] S. A. Almohaimeed and S. Suryanarayanan, "Steady-state analysis of the impact of temperature variations on a distribution transformer," in *2017 North American Power Symposium (NAPS)*, pp. 1–5, 2017.

[17] K. Strunz, *Benchmark Systems for Network Integration of Renewable and Distributed Energy Resources*. 2014.

[18] "Ieee recommended practice and requirements for harmonic control in electric power systems," *IEEE Std 519-2014 (Revision of IEEE Std 519-1992)*, pp. 1–29, 2014.

[19] "Ieee guide for design, operation, and integration of distributed resource island systems with electric power systems," *IEEE Std 1547.4-2011*, pp. 1–54, 2011.

[20] C. Power, *IEEE std 492-2007, Design of Reliable Industrial and Commercial Power Systems (Gold book)*. 2007.

[21] T. Ma, J. Wu, and X. Niu, "Reliability assessment indices and method for urban microgrid," *24th International Conference Exhibition on Electricity Distribution (CIRED)*, no. Jun, pp. 837–840, 2017.

[22] "Ieee recommended practice for establishing liquid-immersed and dry-type power and distribution transformer capability when supplying nonsinusoidal load currents," *IEEE Std C57.110™-2018 (Revision of IEEE Std C57.110-2008)*, pp. 1–68, 2018.

[23] A. van Schijndel, *Power Transformer Reliability Modelling*. PhD thesis, Eindhoven University of Technology, 2010.

[24] "Ieee approved draft standard practices and requirements for semiconductor power rectifier transformers," *IEEE PC57.18.10/D14, Sep 2021*, pp. 1–99, 2021.

[25] H.-C. C. Chun Yao Lee, Hong-Chan Chang, "A method for estimating transformer temperatures and elapsed lives considering operation loads," *WSEAS Transactions on Systems*, pp. 1–123, 2008.

[26] Q. Li, Z. Wang, H. Zhao, H. Liu, L. Tian, X. Zhang, J. Qiu, C. Xue, and X. Zhang, "Research on prediction model of insulation failure rate of power transformer considering real-time aging state," in *2019 IEEE 3rd Conference on Energy Internet and Energy System Integration (EI2)*, pp. 800–805, 2019.

[27] M. C. Chandorkar, D. M. Divan, and R. Adapa, "Control of parallel connected inverters in standalone ac supply systems," *IEEE Transactions on Industry Applications*, vol. 29, pp. 136–143, Jan 1993.

[28] N. Pogaku, M. Prodanovic, and T. C. Green, "Modeling, analysis and testing of autonomous operation of an inverter-based microgrid," *IEEE Transactions on Power Electronics*, vol. 22, pp. 613–625, Mar 2007.

[29] L. Shi, W. Lei, Z. Li, Y. Cui, J. Huang, and Y. Wang, "Stability analysis of digitally controlled dual active bridge converters," *Journal of Modern Power Systems and Clean Energy*, vol. 6, no. 2, pp. 375–383, 2018.

[30] J. Jangra and S. Vadhera, "Load flow analysis for three phase unbalanced distribution feeders using matlab," in *2017 2nd International Conference for Convergence in Technology (I2CT)*, pp. 862–866, 2017.

[31] W. Kersting, "Radial distribution test feeders," *IEEE Transactions on Power Systems*, vol. 6, no. 3, pp. 975–985, 1991.

[32] M. H. Roslan, N. Azis, M. Z. A. A. Kadir, J. Jasni, Z. Ibrahim, and A. Ahmad, "A simplified top-oil temperature model for transformers based on the pathway of energy transfer concept and the thermal-electrical analogy," 2017.